2019 IEEE-RAS 19th International Conference on Humanoid Robots (Humanoids)
Toronto, Canada. October 15-17, 2019

An Adaptive, Humanlike Robot Hand with Selective Interdigitation: Towards Robust Grasping and Dexterous, In-Hand Manipulation

George P. Kontoudis [1], Minas Liarokapis [2], and Kyriakos G. Vamvoudakis [3]

Abstract— **This paper presents an adaptive robot hand that is capable of performing selective interdigitation, robust grasping, and dexterous, in-hand manipulation. The design consists of underactuated, compliant, anthropomorphic robot fingers that are implemented with flexure joints based on elastomer materials (urethane rubber). The metacarpophalangeal (MCP) joint of each finger can achieve both flexion/extension and abduction/adduction. The use of differential mechanisms simplifies the actuation scheme, as we utilize only two actuators for four fingers, achieving affordable dexterity. The two actuators offer increased power transmission during the execution of grasping and manipulation tasks. The importance of the thumb is highlighted with the use of two individual tendon-routing systems for its control. An analytical model is employed to derive the rotational stiffness of the finger flexure joints and select appropriate actuators. Selective interdigitation allows the robot hand to switch from pinch grasp configurations to power grasp configurations optimizing the performance of the device for specific objects. The design can be fabricated with off-the-shelf materials and rapid prototyping techniques, while its efficiency has been validated using an extensive set of experimental paradigms that involved the execution of complex tasks with everyday life objects.**

I. Introduction

Robot grasping and dexterous, in-hand manipulation have received an increased attention over the last decades, as they are the means of intelligent robots to interact with their environment and assist or collaborate with humans in the execution of complex tasks. Robotisists tend to design robot hands seeking inspiration from Nature and try to reproduce the capabilities of the human hand through the development of bio-inspired designs [1]–[4]. This is due to the fact that the human hand is the most dexterous end-effector known, consisting of 29 joints, 27 bones, and more than 123 ligaments that are actuated by more than 30 muscles in a synergistic fashion [5]. The objective of this work is to design and develop an adaptive, anthropomorphic robot hand with a novel actuation mechanism that allows the execution of robust grasping and dexterous in-hand manipulation tasks. We are particularly interested in robot hands that maintain the actuators to fingers ratio below one and yet execute complex, dexterous, in-hand manipulation tasks.

[1]George P. Kontoudis is with the Kevin T. Crofton Department of Aerospace and Ocean Engineering, Virginia Tech, Blacksburg, VA 24060, USA, email: gpkont@vt.edu

[2]Minas Liarokapis is with the New Dexterity research group, Department of Mechanical Engineering, University of Auckland, Auckland, 1010, New Zealand, email: minas.liarokapis@auckland.ac.nz.

[3]Kyriakos G. Vamvoudakis is with the Daniel Guggenheim School of Aerospace Engineering, Georgia Tech, GA 30332, USA, email: kyriakos@gatech.edu.

This work was supported by an NSF CAREER under grant No. CPS-1851588.

Related work: In robotics, several works of multi-fingered, rigid, fully actuated, humanlike robot hands have focused on grasping and dexterous, in-hand manipulation [6]–[8]. However, such devices have certain limitations being heavy, expensive, and difficult to build and maintain. Moreover, these devices require sophisticated sensing elements and complicated control laws. For the control of hand posture, a study [9] revealed that during grasping actions, a higher-level coordination (coupling) in the human hand fingers' motion exists. This study concluded that the first two principal components of the grasp covariance matrix account for approximately 80% of the variance of the total human hand grasping actions. The particular finding inspired new designs of robot hands and control schemes that simplify the execution of everyday grasps. In [10]–[12], the authors presented synergy-based robotic hands for humanlike grasping, where each actuator could trigger a single synergy. This means that the weight of the robotic hand in all cases was increased, while the final force transmitted to the fingers for grasping and manipulation was restricted. In addition, several researchers have relied on dimensionality reduction techniques and other learning methods to simplify the robot hands' operation. In [13], the authors used a similar approach in order to implement synergies in robotics, introducing new representative robot hand grasping strategies called eigengrasps. More precisely, the authors used a dimensionality reduction technique in order to represent the robot hand motion capabilities in low-d manifolds, where the control requirements are relaxed and the task execution is simplified. The derived strategies account again for most of the grasping actions variance and are useful for solving online grasp planning problems.

An alternative to the fully actuated, rigid robot hands is the new class of adaptive robot grippers and hands [14]–[19] that simplify the extraction of robust grasps using structural compliance and underactuation. Adaptive hands can be developed either with flexure joints or with spring loaded pin joints. The elastic elements in the finger structure are typically used for passive extension and the implementation of compliant fingerpads. Although adaptive hands have been extensively used for robust grasping, only few studies have employed them for complex, in-hand manipulation tasks. In [20], the authors proposed the i-HY, an adaptive robot hand that was developed specifically for dexterous manipulation. In this work, the authors achieved dexterous finger interdigitation and finger pivoting, by employing five actuators to control three fingers. This leads to a ratio of 1.66 actuators per finger. The Pisa/IIT SoftHand 2 [21],

978-1-5386-7630-1/19/$31.00 ©2019 IEEE

an anthropomorphic adaptive robot hand employs only two motors, having a ratio of actuators per finger of 0.4. Their design produces motions based on postural synergies [9], manipulation synergies [22], and postural synergies during environmental constraint exploitation [23]. Yet the in-hand manipulation capabilities were limited to rolling of various objects. The work presented in [24] proposes the GR2, a two-fingered adaptive robot hand that performs planar in-hand manipulation, e.g., object rolling and equilibrium point manipulation, with two actuators. The authors in [25] studied in-hand manipulation using a robot hand with a single actuator that exploits extrinsic to the hand resources, such as gravity. Unambiguously, the thumb is the most important finger in grasping and in-hand manipulation tasks [5], [26]. Even hand taxonomies classify human grasp types based on the thumb abduction/adduction [27]. A review that highlights the significance of human thumb is presented in [28].

Contributions: In this paper, we propose a new adaptive, humanlike robot hand that can achieve robust grasping, dexterous, in-hand manipulation (e.g., equilibrium point manipulation and finger pivoting), and selective interdigitation. Interdigitation allows the hand to switch from pinch grasps to power grasps and provide robust grasping performance for specific objects. The robot hand consists of monolithic fingers that make use of flexure joints based on elastomer materials (urethane rubber, Smooth-On PMC-780). The proposed actuation scheme has the ability to perform concurrently flexion/extension and abduction/adduction by employing two actuators in a synergistic fashion. We also compute the rotational stiffness of flexure joints with an analytical model to select the most appropriate actuators. The efficiency of the proposed designs and methods has been validated using a wide range of experiments.

Structure: The remainder of this paper is organized as follows. Section II focuses on the design of the proposed adaptive, humanlike robot hand, Section III discusses the fabrication process of the robot hand, Section IV presents the results of the experimental validation, while section V concludes the paper.

II. Robot Hand Structure

In this section, we focus on the structure of the proposed adaptive, humanlike robot hand. First, we discuss the finger structure and its tendon-routing system. Then, we provide details on the parallel differential mechanisms, that allow for flexion/extension and abduction/adduction on the MCP joint of the four fingers[1]. Next, we present the procedure to achieve anthropomorphism in the proposed robot hand. Moreover, an analytical flexure model is employed for the computation of the rotational flexure joint stiffness.

A. Finger Structure

The structure of the robotic finger is bio-inspired as it uses cables that act as artificial tendons. A comprehensive presentation, modeling, and analysis of the fingers

[1]The four fingers refer to the index, middle, ring, and pinky.

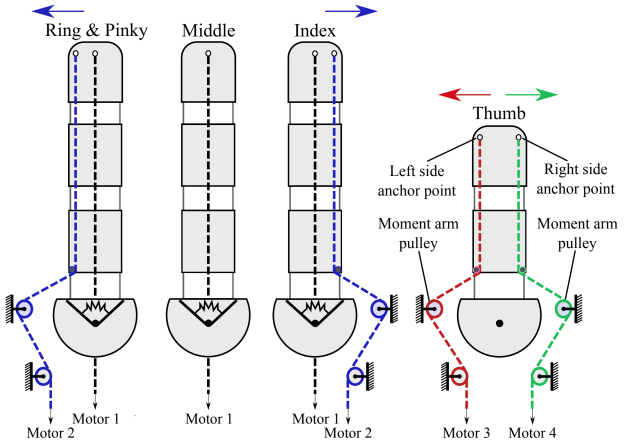

Fig. 1. The finger structure and the tendon-routing system structure. Right-side anchor points enforce clockwise adduction. Left-side anchor points impose counterclockwise adduction. Both sides anchor points allow for bi-directional motion.

incorporated into the proposed robot hand can be found in [29], [30]. The four fingers consist of distal, middle, and proximal phalanges, while the thumb comprises of a distal and a proximal phalange, as shown in Fig. 1. The portions of fingers with smaller width, which are illustrated in white, represent the flexure joints. These joints realize the flexion/extension motion. The circular base allows for abduction/adduction on the MCP joint. A torsional spring is responsible for keeping the finger to its rest position and for mechanically implementing the abduction motion. The fingers are attached to the hand through the MCP joint. This is achieved with a single bolt-nut set for each finger, which makes the design modular. The second actuation system of the index, ring, and pinky fingers accomplishes initially the adduction/abduction motion of the MCP joint and then triggers the flexion/extension of each finger. This twofold contribution of the second actuation system is due to the design choice to place the anchor point at the side of the distal phalange.

Anchor points and moment arm pulleys for each separate tendon-routing system were selected according to the mechanical behavior desired. One can notice that from the natural position of the human hand, index's adduction has an opposite movement from ring and pinky fingers. The adduction motion from the natural position of the middle finger can be neglected since it is relatively small. On the other hand, the thumb's motion includes bidirectional abduction/adduction. Therefore, for the anthropomorphic (right) hand we are able to produce 3 different MCP joint movements with respect to the human hand's motion. For this purpose, we employ right-side anchor points for clockwise motion, left-side anchor points for counterclockwise motion, and both-sides anchor points for bidirectional rotation. In case we pursue single side rotation, central anchor points utilization is imposed to actuate the finger's flexion/extension movements. The significance of the thumb is emphasized with two individual tendon-routing systems that achieve both concurrently and individually flexion/extension and ab-

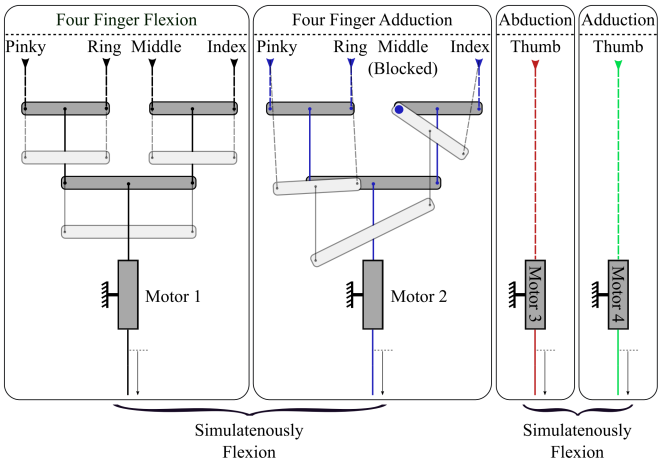

Fig. 2. The actuation scheme of the robot hand. One differential mechanism implements flexion/extension to the four fingers. Another differential mechanism realizes abduction/adduction on the MCP joint of the four fingers. Individual motors are assigned to the adduction and abduction motions of the thumb. Simultaneous actuation of the differential mechanisms results to flexion at the current adduction angle. Similarly, concurrent actuation of the thumb motors realizes flexion at the specific adduction angle.

duction/adduction. Since the thumb employs two individual tendon-routing systems, no torsional spring is required.

B. Actuation Scheme

We equip the robot hand with an actuation scheme that comprises of four tendon-routing systems and two parallel differential mechanisms based on the Whiffletree, as presented in Fig. 2. More specifically, we employ one differential mechanism for the flexion/extension of the four digits and another parallel differential mechanism for the abduction/adduction of the four digits. The second differential mechanism is based on the lockable Whiffletree as presented in [17] and it also endows the flexion after the maximum adduction of the MCP joint. The contribution of the second motor to the flexion motion augments the force distribution among fingers. We select a three-bar structure and not a two-bar (i.e. index directly connected to the main bar), because we seek to distribute the exerted forces to the three fingers. In case of a two-bar differential mechanism the exerted force of the index would be similar with the cumulative exerted forces of the ring and pinky. Note that in this work we employ a pin to constantly block the abduction/adduction of the middle finger, rather than using buttons to selectively lock the finger motion [17]. We select lever-based differential mechanisms because they are simple to design, easy to fabricate, and lightweight comparing to gear-based mechanisms. The rest two tendon-routing systems are dedicated to the thumb abduction and the thumb adduction. The ratio of actuators per finger is 0.8. That is higher from the Pisa/IIT Soft Hand 2 which has 0.4 [21] and lower than the i-HY hand which has 1.66 [20].

The synergistic collaboration of actuators switches between flexion and adduction motions. More precisely, when both tendon-routing systems of the thumb are simultaneously actuated, then thumb flexion occurs preserving the desired adduction angle. Similarly, when both differential mechanisms are simultaneously actuated, then flexion of the four fingers occurs at the current adduction angle. Note that the lateral motion is not purely adduction but also includes some flexion. In particular, the fingers first perform adduction and then a combination of adduction and flexion motions. Therefore, the differential mechanism for adduction can be used for precision grasping without even actuating the middle finger, as it is blocked in that motion. That is a useful functionality for in-hand manipulation actions. A detailed analysis of the reachable workspace for a single finger with the employed actuation mechanism is presented in [30].

The flexion/extension is the dominant motion of the fingers for the vast majority of grasping and in-hand manipulation tasks. Thus, we design the actuation scheme in a way that allows flexion/extension at every configuration. In addition, we equip the robot hand with fingers capable of performing lateral motion on the MCP joint, which prevails in various hand synergies. The abduction/adduction motion on the MCP joint highly appears in both the first and the second principal components as presented in [9]. Another study of hand synergies during environmental exploitation [23] reports that the abduction/adduction of the MCP joint of the four fingers and the thumb is realized with the first and the second synergy respectively. Interestingly, the underlying synergies for in-hand manipulation tasks vary significantly, depending on the task [22]. Yet, a combination of abduction/adduction on the MCP joint appears in the first and the second synergies of all the in-hand manipulation tasks. In fact, this reveals that the lateral motion of the MCP joint is valuable not only for robust grasping, but also for dexterous, in-hand manipulation tasks.

C. Anthropomorphism

The proposed robot hand is anthropomorphic both in structure and in kinematics. For the hand structure we use anthropometry studies while for the kinematics we utilize human hand medical tests (Kapandji test). Moreover, we design the finger joints such that their range of motion is similar with the human hand. The structure of the robot hand was derived by using hand anthropometry studies [31]. This work provides an estimation of the human hand joint centers, the bone lengths, the spatial location of the MCP joint for the four fingers, and the spatial location of the thumb carpometacarpal (CMC) joint based on the hand dimensions. The required hand dimensions are the hand length and the hand breadth. First, the joint centers and the bone lengths were used to derive the finger dimensions. Then, the spatial location of the four fingers along with the hand length and the hand breadth were employed to design the palm. The thumb structure follows the paradigm presented in our previous work [17], [32].

The kinematics of the robot hand depend on the motion of the fingers. We design the joints in a way that conforms to the Kapandji test [5]. More specifically, the Kapandji test consists of two stages: 1) the thumb's fingertip must be able to contact with the MCP base frames of the index, middle,

TABLE I

FINGER STRUCTURE OF ROBOT HAND

Finger	*Weight*	*Length*	*Breadth*	*Width*	*Adduction*
Index	25 g	88 mm	16.2 mm	15 mm	27.3°
Middle	25 g	98 mm	16.2 mm	15 mm	Fixed
Ring	25 g	95 mm	16.2 mm	15 mm	-18.2°
Pinky	20 g	76 mm	16.2 mm	15 mm	-30.1°
Thumb	20 g	68 mm	16.2 mm	15 mm	±165°

TABLE II

FINGER JOINT ROTATIONAL FLEXURE STIFFNESS

Stiffness $\left[\frac{\text{N.mm}}{\text{deg}}\right]$	Index	Middle	Ring	Pinky	Thumb
DIP - Flexion	1.25	1.25	1.25	1.25	1.25
PIP - Flexion	1.25	1.25	1.25	1.25	0.65
MCP - Flexion	0.65	0.65	0.65	0.65	-
MCP - Adduction	0.50	0.50	0.50	0.50	Bidirection

ring, and pinky fingers; and 2) the thumb's fingertip must be able to contact the index and pinky fingertips, without any flexion on the proximal interphalangeal (PIP) joint and the distal interphalangeal (DIP) joint. This test is developed for evaluating the post-surgery dexterity of a human hand and provides a quick and robust experimental validation of the human hand function.

D. Smooth Curvature Model

The proposed robot hand comprises of 14 flexure joints and 5 pin joints. The flexure joints are responsible for the flexion/extension, while the pin joints realize the abduction/adduction in all fingers. The flexure joints introduce compliance to the design and thus they are critical for the adaptability of the hand. Pin joints for underactuated fingers were extensively studied in the literature [33]. Yet, the modeling of flexure joints is more challenging.

For the stiffness computation of the flexure joints we use the smooth curvature model [34] that is an approximation of the Euler-Bernoulli large bending model and make use of only three parameters. An analytical example of the rotational stiffness flexure joint computation is provided in [30]. We consider the case of a flexure joint being subject to large loads and buckling. Although we do not have an external load to apply vertical forces to the fingers, the tendon develops such forces due to its routing. The Euler's critical load equation describes the buckling as,

$$P_{\text{cr}} = \frac{\pi^2 E_{\text{flex}} I_{\text{flex}}}{4 L_{\text{flex}}^2}, \tag{1}$$

where E_{flex} is the Young's modulus, I_{flex} is the moment of inertia, and L_{flex} is the length of the flexure joint. The moment of inertia of a rectangular area is given by, $I_{\text{flex}} = \frac{bh^3}{12}$, where b is the flexure width and h is the flexure thickness. We assume that the Young's modulus is constant. Therefore, the symmetric global stiffness matrix yields,

$$\mathbf{K}_{\text{flex}} = \frac{E_{\text{flex}} I_{\text{flex}}}{L_{\text{flex}}} \begin{bmatrix} \frac{12-\pi^2}{12} & \frac{1}{12} & \frac{1}{60} \\ \frac{1}{12} & \frac{360-\pi^2}{360} & 0 \\ \frac{1}{60} & 0 & \frac{4200-\pi^2}{4200} \end{bmatrix}. \tag{2}$$

To associate the rotational flexure stiffness to the global stiffness matrix $\mathbf{K}_{\text{flex}}$ and without loss of generality, we assume straight curvature $\kappa = 0$ when then flexure joint is flexed in the free space [35]. To this end, the final rotational flexure stiffness under large load and buckling is related to the first element in (2) which results to,

$$k_{\text{flex}}^{\text{rot}} = \frac{12-\pi^2}{12} \frac{E_{\text{flex}} \frac{bh^3}{12}}{L_{\text{flex}}} = 0.0148 \frac{E_{\text{flex}} b h^3}{L_{\text{flex}}}. \tag{3}$$

The effect of the flexure joint thickness h is of paramount importance to the stiffness $k_{\text{flex}}^{\text{rot}}$, as it is proportional to its cubic order.

III. INFORMED DESIGN AND FABRICATION PROCESS

In this section, we compute specific characteristics of the proposed device using methods that where described in the previous section. Next, we present the process to fabricate the robot hand as well as its final characteristics.

A. Hand Design

We develop a robot hand based on hand length $L_{\text{H}} = 185$ mm and hand breadth $B_{\text{H}} = 90$ mm. The link lengths of the fingers follow the anthropometric models described in [31]. The finger dimensions are provided in Table I. We approximate the finger weight from the urethane rubber specifications given by the manufacturer (Smooth-On PMC-780). The total weight of each finger varies from 20 g to 25 g. Next, we place the moment arm pulleys to produce the desired adduction angles [36]. The moment arm pulley position analysis is discussed in [30].

The kinematics of the fingers depend on the width of the the PIP, the DIP, and the MCP flexure joint. We select the width of the joints experimentally, by following the Kapandji test [5]. Since we have already selected the finger width we follow the analysis in Subsection II-D to derive the stiffness of each joint. The final results are depicted in Table II. Then, we relate the stiffness of the flexure joints with the stiffness of the torsional spring. More specifically, the torsional spring needs to be have enough stiffness to mechanically rebound the finger to its initial position and to concurrently counteract gravity. On the other hand, it should be soft enough to allow the abduction/adduction when the tendon shifts, otherwise the flexion/extension dominates. The resulting torsional spring stiffness follows the analysis in [30]. The MCP joint of the thumb performs abduction/adduction without the need of a torsional spring, as we employ side anchor points for the tendon-routing systems.

B. Fabrication Process

For the fabrication process of the proposed adaptive robot hand, we employed exclusively off-the-shelf materials that can be easily found in hardware stores around the world. The

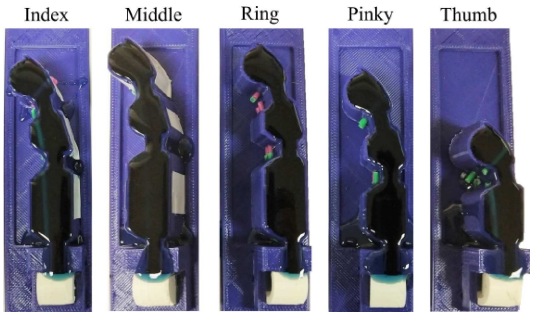

Fig. 3. The five fingers during the curing phase of the elastomer material. We used the Hybrid Deposition Manufacturing technique that combines 3D printed and elastomer materials. The fingers are monolithic and made out of urethane rubber, while the rotating base is made out of ABS material.

anthropomorphic fingers are monolithic and they are fabricated with urethane rubber of shore hardness 80 A (Smooth-On PMC-780), using the Hybrid Deposition Manufacturing (HDM) technique [37]. The HDM makes use of a reusable mold (blue), a rotating base (white), and a sacrificial mold (blue with white tape), as presented in Fig. 3. The reusable mold accommodates the sacrificial mold and the rotating base to prevent elastomer leakage during the curing phase. The design incorporates modular fingers into the hand.

In Fig. 4, we present the adaptive robot hand in four views. The side view depicts the two parallel differential mechanisms for the flexion/extension and abduction/adduction of the four fingers. The rotating base of the MCP joint is shown in white in the back view. In Table III, the characteristics of the robot hand are presented. The palm was exclusively fabricated from 3D printed ABS material. The total weight of the proposed hand including the motors is 650 g. The net weight of the hand without the motors is 360 g, allowing for further weight reduction. The adaptive hand is lightweight due to the monolithic elastomer fingers, the lever-based differential mechanisms, and the underactuated structure. The actuation scheme provides a variety of motions to the robot hand. More specifically, for a right hand, the thumb achieves clockwise (CW) and counterclockwise (CCW) abduction/adduction (A/A) and flexion/extension (F/E), the index CW abduction/adduction and flexion/extension, the ring and the pinky CCW abduction/adduction and flexion/extension, and the middle flexion/extension. The design is open-source and all the files that are required for the replication and the control of the proposed actuation mechanism are freely available through the OpenBionics initiative website [2].

C. Actuator Selection

Next, we compute the required tendon force for each actuator by utilizing the analysis in [30]. The required tendon force for flexion and adduction takes the form of,

$$f_{a_f} = \frac{k_d \Delta\theta_d}{r_d} = \frac{k_p \Delta\theta_p}{r_p} = \frac{k_{fm} \Delta\theta_{fm}}{r_{fm}}, \quad (4)$$

$$f_{a_a} = \frac{k_t \Delta\theta_{MCP}}{r_{am}}, \quad (5)$$

[2] www.openbionics.org

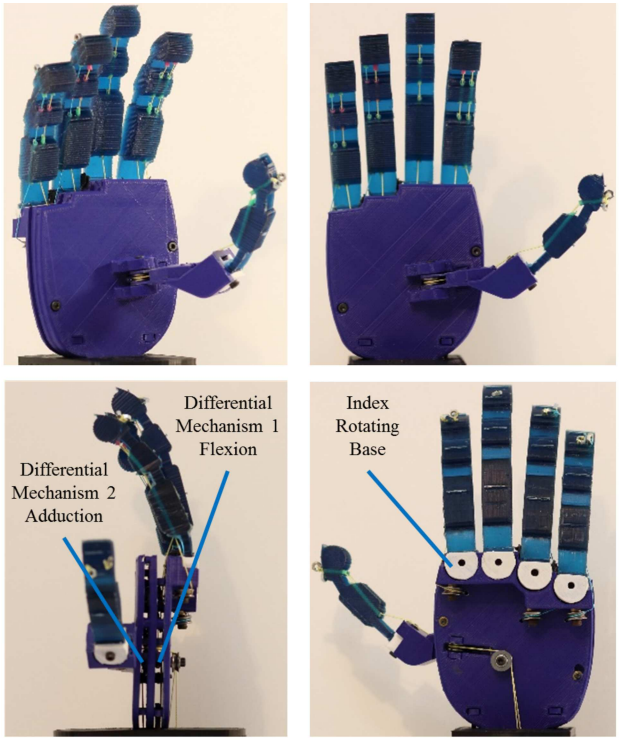

Fig. 4. The adaptive robot hand in various views. The two parallel differential mechanisms for flexion/extension and abduction/adduction are demonstrated in the side view. Lever-based differential mechanisms reduce the fabrication complexity and the weight. The rotating bases of the MCP joint for the abduction/adduction are illustrated in white.

where k_d, k_p, k_{fm}, k_t are the stiffness of the DIP, the PIP, the flexion MCP, and the adduction MCP joint respectively. The $\Delta\theta_d$ $\Delta\theta_p$, $\Delta\theta_{fm}$, $\Delta\theta_{MCP}$ are the configurations of the DIP, the PIP, the flexion MCP, and the adduction MCP joint respectively. The r_d, r_p, r_{fm}, and r_{am} are the pulley radii of the DIP, PIP, flexion MCP, and adduction MCP joints respectively. The desired flexion angles of each joint are 77^o for the DIP joint, 93^o for the PIP joint, and 72^o for the flexion MCP joint, as presented in [38]. Yet, due to palm restrictions the maximum attained MCP joint angle is 60^o. Also, we employ by design a DIP rest angle of 20^o from [5]. To this end the DIP joint operates from 20^o to 90^o, i.e. 70^o. Therefore, the achieved angles are 70^o for the DIP joint, 90^o for the PIP joint, and 60^o for the flexion MCP joint. The attained adduction angles are provided in Table I.

TABLE III
ROBOT HAND CHARACTERISTICS

Dimensions	$L_H = 185$ mm, $B_H = 90$ mm
Weight	650 g (with motors), 360 g (net)
Motors	4 Dynamixel RX-28, 2.8 Nm at 12V
Software	ROS
Materials	3D printed ABS; Smooth-On PMC-780
Availability	Open-source
Cost	$ 1,000
Motions	Thumb: CW - CCW A/A, F/E; Index: CW A/A, F/E; Middle: F/E; Ring & Pinky: CCW A/A, F/E

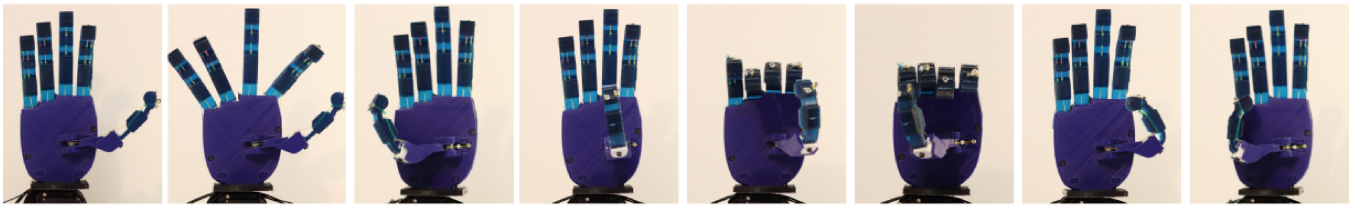

Fig. 5. Grasping postures and gestures executed by the proposed adaptive robot hand. The abduction/adduction capabilities are depicted in the first four images. The last four images show the implementation of the Kapandji test.

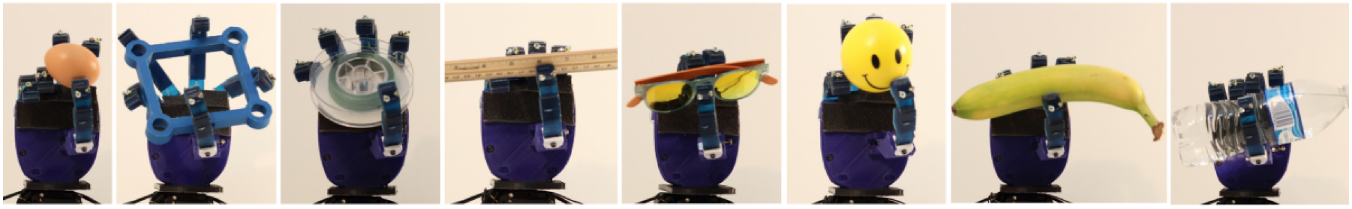

Fig. 6. The proposed adaptive robot hand while performing grasping experiments with various everyday life objects. More precisely, the grasps involve an egg, a large rectangular object, a plastic cylindrical object, a ruler, a pair of sunglasses, a small plastic ball, a banana, and a bottle of water.

The required force for the flexion of the four fingers is, $f_{\mathrm{a_{f,total}}} = f_{\mathrm{a_{f,index}}} + f_{\mathrm{a_{f,middle}}} + f_{\mathrm{a_{f,ring}}} + f_{\mathrm{a_{f,pinky}}} = 70$ N, where for each finger $f_{\mathrm{a_{f,}}i} = f_{\mathrm{a_{f,}}i\mathrm{,DIP}} + f_{\mathrm{a_{f,}}i\mathrm{,PIP}} + f_{\mathrm{a_{f,}}i\mathrm{,MCP}}$. Similarly, the required tendon force for the adduction of the three fingers is, $f_{\mathrm{a_{a,total}}} = f_{\mathrm{a_{a,index}}} + f_{\mathrm{a_{a,ring}}} + f_{\mathrm{a_{a,pinky}}} = 8$ N, where for each finger $f_{\mathrm{a_{a,}}i} = f_{\mathrm{a_{a,}}i\mathrm{,MCP}}$. We equip the robot hand with 4 Dynamixel RX-28 servo motors with torque $T_{\mathrm{m}} = 2.8$ Nm at 12V and outer shaft diameter $D_{\mathrm{m}} = 0.0025$ m. We place a pulley to the outer shaft with diameter $D_{\mathrm{p}} = 0.0500$ m. The resulting tendon force of each actuator is $f_{\mathrm{a}} = 112$ N. Since two actuators are contributing to the flexion, the four fingers can easily perform full flexion. It must be noted that we use high torque motors to achieve significant exerted forces at every configuration.

IV. Results and Experiments

In this section, we present various experiments to validate the efficiency of the proposed adaptive robot hand. First, we show the feasible robot hand gestures and we perform a medical test to validate the humanlikeness of the design. Next, we conduct extended grasping experiments with everyday life objects. Finally, we perform equilibrium point manipulation and finger pivoting experiments to demonstrate the in-hand manipulation capabilities of the proposed device. All experiments were recorded and can be found in [39].

A. Hand Postures and Gestures

In this subsection, we perform experiments with the developed robot hand to examine its anthropomorphic characteristics. In the first four images of Fig. 5, all the possible robot hand grasping postures and gestures are presented, while in the last four images of Fig. 5, we present the results of the Kapandji test [5]. It can be easily noticed, that the fingertip of the thumb is able to contact the fingertips of the index and the pinky fingers, as well as their base frames, thus the Kapandji test was successfully performed. In Fig. 7, we show

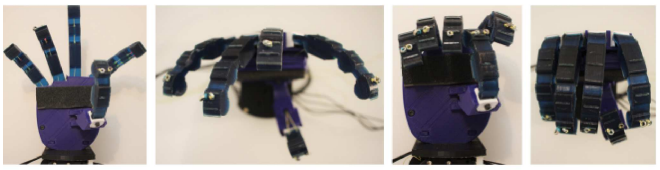

Fig. 7. Finger interdigitation of the thumb with the index and middle fingers. The adduction of the MCP joint in the four fingers is shown in the first two images. This allows the finger interdigitation of the thumb with the index and middle fingers, as presented in the last two images.

Fig. 8. A switch from pinch to power grasp. The first two images depict the pinch grasp and the last two images the power grasp. The execution of this task is facilitated by the finger interdigitation.

the interdigitation capabilities of the robot hand. Particularly, the adduction of the MCP joint of the four fingers (first two images of the Fig. 7) allows the placement of the thumb finger at the intermediate to the index and the middle fingers as shown in the first two columns of Fig. 7. This is a powerful motion that allows switching from pinch to power grasps.

B. Grasping Everyday Life Objects

In order to experimentally validate the efficiency of the proposed adaptive robot hand and assess its grasping capabilities, we chose to conduct a wide range of experiments involving a series of everyday objects such as an egg, a 3D printed rectangular shape, a plastic cylindrical shape, a ruler, a pair of sunglasses, a small plastic ball, a banana, and bottle of water. Representative grasps with the examined set of objects are presented in Fig. 6. It is evident that the

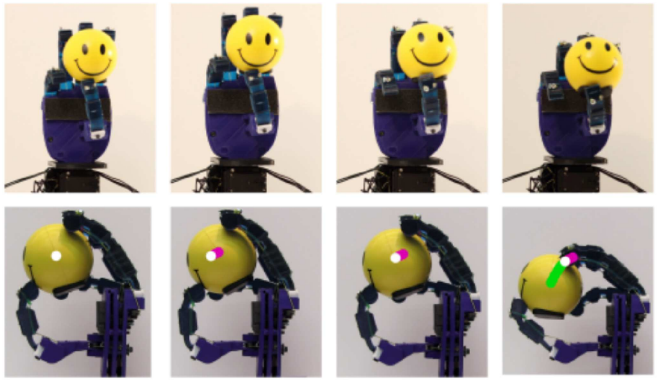

Fig. 9. An equilibrium point manipulation experiment executed with the proposed robot hand. The robot hand successfully grasps a spherical object and then performs rolling of the object that results to an equilibrium point motion.

underactuation and the structural compliance of the proposed adaptive robot hand facilitates the grasping and handling of delicate and/or fragile objects, e.g., the raw egg and the pair of sunglasses, without breaking them.

C. Dexterous Manipulation

The proposed adaptive, humanlike robot hand is capable of executing not only robust grasps but also dexterous, in-hand manipulation tasks using only four actuators. In particular, the hand is able to perform equilibrium point manipulation motions as well as finger pivoting motions. An example of an equilibrium point manipulation task executed with a small plastic ball, is depicted in Fig. 9. The robot hand rolls the object, yet the rolling is not simple and results also to equilibrium point manipulation motion. The initial equilibrium point position is illustrated in white. The first equilibrium point motion is depicted in pink as shown in the second column of Fig. 9. The major equilibrium point motion is illustrated in green in the last column of Fig. 9. In Fig. 10, the finger pivoting of a highlighter pen is presented. First, the highlighter pen is grasped with the index and thumb fingers, yet without any contact of the rest fingers as shown in the first two images of Fig. 10. This can be achieved by mainly using the adduction differential mechanism for flexion as noted in Subsection II-B. Then, the pen is pivoted by the flexion of the middle and ring fingers as depicted in the third image of Fig. 10. Lastly, the pen is re-oriented within the hand by utilizing the adduction differential mechanism and the thumb. Finger pivoting is one of the most challenging dexterous in-hand manipulation tasks.

V. Conclusions

This paper focused on the modeling, analysis, and development of an adaptive, humanlike robot hand that is able to achieve selective interdigitation, robust grasping and dexterous, in-hand manipulation of everyday objects. The hand consists of adaptive, anthropomorphic robot fingers implemented with flexure joints and an MCP spring loaded joint that can implement both flexion/extension and abduction/adduction concurrently. Differential mechanisms are used to simplify the actuation scheme, utilizing only two actuators for four fingers. An analytical model is proposed for the computation of the finger flexure joint rotational stiffness and the selection of the actuators. The hand can be replicated using off-the-shelf materials and rapid prototyping techniques, while its efficiency has been validated using an extensive set of experimental paradigms. Selective interdigitation allows the proposed adaptive robot hand to switch from pinch to power grasp configurations highlighting its grasping performance for various objects. The anthropomorphic adaptive robot hand maintains an actuators to fingers ratio below one, achieving rolling with equilibrium point manipulation and finger pivoting with object re-orientation. The latter is considered as one of the most complex dexterous, in-hand manipulation tasks.

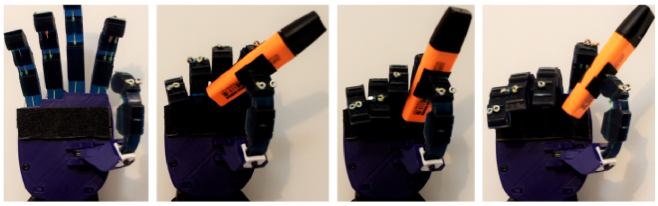

Fig. 10. The finger pivoting is responsible for the internal rotation of the highlighter pen. The proposed device has also the ability to re-orient objects within the hand.

References

[1] S. A. Dalley, T. E. Wiste, T. J. Withrow, and M. Goldfarb, "Design of a multifunctional anthropomorphic prosthetic hand with extrinsic actuation," *IEEE/ASME Transactions on Mechatronics*, vol. 14, no. 6, pp. 699–706, 2009.

[2] A. D. Deshpande, Z. Xu, M. J. V. Weghe, B. H. Brown, J. Ko, L. Y. Chang, D. D. Wilkinson, S. M. Bidic, and Y. Matsuoka, "Mechanisms of the anatomically correct testbed hand," *IEEE/ASME Transactions on Mechatronics*, vol. 18, no. 1, pp. 238–250, 2013.

[3] C.-H. Xiong, W.-R. Chen, B.-Y. Sun, M.-J. Liu, S.-G. Yue, and W.-B. Chen, "Design and implementation of an anthropomorphic hand for replicating human grasping functions," *IEEE Transactions on Robotics*, vol. 32, no. 3, pp. 652–671, 2016.

[4] Z. Xu and E. Todorov, "Design of a highly biomimetic anthropomorphic robotic hand towards artificial limb regeneration," in *IEEE International Conference on Robotics and Automation*, 2016, pp. 3485–3492.

[5] A. Kapandji, "Cotation clinique de l'opposition et de la contre-opposition du pouce," in *Annales de Chirurgie de la Main*, vol. 5, no. 1. Elsevier, 1986, pp. 67–73.

[6] C. Lovchik and M. A. Diftler, "The robonaut hand: A dexterous robot hand for space," in *IEEE International Conference on Robotics and Automation*, vol. 2, 1999, pp. 907–912.

[7] J. Butterfaß, M. Grebenstein, H. Liu, and G. Hirzinger, "DLR-Hand II: Next generation of a dextrous robot hand," in *IEEE International Conference on Robotics and Automation*, vol. 1, 2001, pp. 109–114.

[8] H. Kawasaki, T. Komatsu, and K. Uchiyama, "Dexterous anthropomorphic robot hand with distributed tactile sensor: Gifu hand II," *IEEE/ASME Transactions on Mechatronics*, vol. 7, no. 3, pp. 296–303, 2002.

[9] M. Santello, M. Flanders, and J. F. Soechting, "Postural hand synergies for tool use," *Journal of Neuroscience*, vol. 18, no. 23, pp. 10 105–10 115, 1998.

[10] C. Y. Brown and H. H. Asada, "Inter-finger coordination and postural synergies in robot hands via mechanical implementation of principal components analysis," in *IEEE/RSJ International Conference on Intelligent Robots and Systems*, 2007, pp. 2877–2882.

[11] K. Xu, H. Liu, Y. Du, and X. Zhu, "Design of an underactuated anthropomorphic hand with mechanically implemented postural synergies," *Advanced Robotics*, vol. 28, no. 21, pp. 1459–1474, 2014.
[12] M. G. Catalano, G. Grioli, E. Farnioli, A. Serio, C. Piazza, and A. Bicchi, "Adaptive synergies for the design and control of the Pisa/IIT SoftHand," *The International Journal of Robotics Research*, vol. 33, no. 5, pp. 768–782, 2014.
[13] M. T. Ciocarlie and P. K. Allen, "Hand posture subspaces for dexterous robotic grasping," *The International Journal of Robotics Research*, vol. 28, no. 7, pp. 851–867, 2009.
[14] S. Hirose and Y. Umetani, "The development of soft gripper for the versatile robot hand," *Mechanism and Machine Theory*, vol. 13, no. 3, pp. 351–359, 1978.
[15] A. M. Dollar and R. D. Howe, "The highly adaptive SDM hand: Design and performance evaluation," *The International Journal of Robotics Research*, vol. 29, no. 5, pp. 585–597, 2010.
[16] D. M. Aukes, B. Heyneman, J. Ulmen, H. Stuart, M. R. Cutkosky, S. Kim, P. Garcia, and A. Edsinger, "Design and testing of a selectively compliant underactuated hand," *The International Journal of Robotics Research*, vol. 33, no. 5, pp. 721–735, 2014.
[17] G. P. Kontoudis, M. V. Liarokapis, A. G. Zisimatos, C. I. Mavrogiannis, and K. J. Kyriakopoulos, "Open-source, anthropomorphic, underactuated robot hands with a selectively lockable differential mechanism: Towards affordable prostheses," in *IEEE/RSJ International Conference on Intelligent Robots and Systems*, 2015, pp. 5857–5862.
[18] M. Ciocarlie, F. M. Hicks, R. Holmberg, J. Hawke, M. Schlicht, J. Gee, S. Stanford, and R. Bahadur, "The Velo gripper: A versatile single-actuator design for enveloping, parallel and fingertip grasps," *The International Journal of Robotics Research*, vol. 33, no. 5, pp. 753–767, 2014.
[19] M. Controzzi, F. Clemente, D. Barone, A. Ghionzoli, and C. Cipriani, "The SSSA-MyHand: A dexterous lightweight myoelectric hand prosthesis," *IEEE Transactions on Neural Systems and Rehabilitation Engineering*, vol. 25, no. 5, pp. 459–468, 2017.
[20] L. U. Odhner, L. P. Jentoft, M. R. Claffee, N. Corson, Y. Tenzer, R. R. Ma, M. Buehler, R. Kohout, R. D. Howe, and A. M. Dollar, "A compliant, underactuated hand for robust manipulation," *The International Journal of Robotics Research*, vol. 33, no. 5, pp. 736–752, 2014.
[21] C. Della Santina, C. Piazza, G. Grioli, M. G. Catalano, and A. Bicchi, "Toward dexterous manipulation with augmented adaptive synergies: The Pisa/IIT SoftHand 2," *IEEE Transactions on Robotics*, no. 99, pp. 1–16, 2018.
[22] E. Todorov and Z. Ghahramani, "Analysis of the synergies underlying complex hand manipulation," in *IEEE International Conference of the Engineering in Medicine and Biology Society*, 2004, pp. 4637–4640.
[23] C. Della Santina, M. Bianchi, G. Averta, S. Ciotti, V. Arapi, S. Fani, E. Battaglia, M. G. Catalano, M. Santello, and A. Bicchi, "Postural hand synergies during environmental constraint exploitation," *Frontiers in neurorobotics*, vol. 11, p. 41, 2017.
[24] N. Rojas, R. R. Ma, and A. M. Dollar, "The GR2 gripper: An underactuated hand for open-loop in-hand planar manipulation," *IEEE Transactions on Robotics*, vol. 32, no. 3, pp. 763–770, 2016.
[25] N. C. Dafle, A. Rodriguez, R. Paolini, B. Tang, S. S. Srinivasa, M. Erdmann, M. T. Mason, I. Lundberg, H. Staab, and T. Fuhlbrigge, "Extrinsic dexterity: In-hand manipulation with external forces," in *IEEE International Conference on Robotics and Automation*, 2014, pp. 1578–1585.
[26] E. Poydebat, M. Laurin, P. Gorce, and V. Bels, "Evolution of grasping among anthropoids," *Journal of evolutionary biology*, vol. 21, no. 6, pp. 1732–1743, 2008.
[27] T. Feix, J. Romero, H.-B. Schmiedmayer, A. M. Dollar, and D. Kragic, "The GRASP taxonomy of human grasp types," *IEEE Transactions on Human-Machine Systems*, vol. 46, no. 1, pp. 66–77, 2016.
[28] V. K. Nanayakkara, G. Cotugno, N. Vitzilaios, D. Venetsanos, T. Nanayakkara, and M. N. Sahinkaya, "The role of morphology of the thumb in anthropomorphic grasping: a review," *Frontiers in Mechanical Engineering*, vol. 3, p. 5, 2017.
[29] G. P. Kontoudis, M. Liarokapis, and K. G. Vamvoudakis, "A compliant, underactuated finger for anthropomorphic hands," in *IEEE International Conference on Rehabilitation Robotics*, 2019, pp. 682–688.
[30] G. P. Kontoudis, M. Liarokapis, K. G. Vamvoudakis, and T. Furukawa, "An adaptive actuation mechanism for anthropomorphic robot hands," *Frontiers in Robotics and AI*, vol. 6, p. 16, 2019.
[31] B. Buchholz, T. J. Armstrong, and S. A. Goldstein, "Anthropometric data for describing the kinematics of the human hand," *Ergonomics*, vol. 35, no. 3, pp. 261–273, 1992.
[32] M. V. Liarokapis, P. K. Artemiadis, and K. J. Kyriakopoulos, "Quantifying anthropomorphism of robot hands," in *IEEE International Conference on Robotics and Automation*, 2013, pp. 2041–2046.
[33] L. Birglen, T. Laliberté, and C. M. Gosselin, *Underactuated robotic hands*. Springer, 2007.
[34] L. U. Odhner and A. M. Dollar, "The smooth curvature model: An efficient representation of Euler–Bernoulli flexures as robot joints," *IEEE Transactions on Robotics*, vol. 28, no. 4, pp. 761–772, 2012.
[35] J. Guo and K.-M. Lee, "Compliant joint design and flexure finger dynamic analysis using an equivalent pin model," *Mechanism and Machine Theory*, vol. 70, pp. 338–353, 2013.
[36] R. Degeorges and C. Oberlin, "Measurement of three-joint-finger motions: Reality or fancy? A three-dimensional anatomical approach," *Surgical and Radiologic Anatomy*, vol. 25, no. 2, pp. 105–112, 2003.
[37] R. R. Ma, J. T. Belter, and A. M. Dollar, "Hybrid deposition manufacturing: Design strategies for multimaterial mechanisms via three-dimensional printing and material deposition," *Journal of Mechanisms and Robotics*, vol. 7, no. 2, p. 021002, 2015.
[38] G. Bain, N. Polites, B. Higgs, R. Heptinstall, and A. McGrath, "The functional range of motion of the finger joints," *Journal of Hand Surgery (European Volume)*, vol. 40, no. 4, pp. 406–411, 2015.
[39] G. P. Kontoudis, M. Liarokapis, and K. G. Vamvoudakis, "Adaptive robot hand for robust grasping, and dexterous, in-hand manipulation," Retrieved from: https://youtu.be/wvo0tKD7eJ8, September 2019.